JOURNAL OF SOLID STATE CHEMISTRY 98, 159–173 (1992)

Electron Paramagnetic Resonance Investigation of the Cr(VI) to Cr(V) and/or Cr(III) Thermal Reductions in Single Crystals of CrO_4^{2-}-doped M_2SnCl_6 (M = NH_4^+, K^+, $CH_3NH_3^+$, and $[(CH_3)_2NH_2]^+$)

JIANG-TSU YU, CHING-JIUN WU, SSU-HAO LOU, AND MEI-NA TSAI

Institute of Physics, National Taiwan Normal University, Taipei 11718, Taiwan, Republic of China

Received August 21, 1991; in revised form October 30, 1991

We have performed a series of EPR measurements on M_2SnCl_6 (M = NH_4^+, $CH_3NH_3^+$, and $[(CH_3)_2NH_2]^+$) crystals doped with the CrO_4^{2-} ion and thermally treated at different temperatures. Via EPR, we have detected the Cr(VI)O_4^{2-} to Cr(V) and/or Cr(III) thermal reductions. A Cr(V) species, in the form of CrO_4^{3-}, is thermally produced in $(NH_4)_2SnCl_6$ and in K_2SnCl_6 co-doped with NH_4^+. We tentatively assign the thermally produced Cr(III) species as isolated Cr^{3+} ions. We have also studied in some detail the Cr(VI) to Cr(III) thermal reduction in K_2SnCl_6 : CrO_4^{2-} crystals either co-doped with one of the $[(CH_3)_nNH_{4-n}]^+$ ions (n = 0–4) or coated with $CH_3NH_2 \cdot HCl$ or NH_4Cl. The experimental results indicate that it is the hydrogens of the N–H groups which are responsible for the observed reduction. We have analyzed the magnetic symmetries and the spin Hamiltonian parameters of the thermally produced Cr(V) and Cr(III) species. These species can be controllably and repeatably produced via thermal treatments. This thermal method provides an attractive and easily accessible method for the production of the CrO_4^{3-} species, which is conventionally produced via either X- or γ-ray irradiation. © 1992 Academic Press, Inc.

Introduction

This paper reports the investigations by electron paramagnetic resonance (EPR) of the thermal reductions of Cr(VI) into Cr(V) and/or Cr(III) in single crystals of M_2SnCl_6 (M = NH_4^+, K^+, $CH_3NH_3^+$, and $[(CH_3)_2NH_2]^+$) doped with CrO_4^{2-}. The thermal reduction of Cr(VI) into Cr(V), in the form of a Cr(V) oxyanion, has been observed in $(NH_4)_2SnCl_6$ and in K_2SnCl_6 co-doped with NH_4^+. The thermal reduction of Cr(VI) into Cr(III) has been observed in the following CrO_4^{2-}-doped crystals: (a) $(NH_4)_2SnCl_6$; (b) K_2SnCl_6 co-doped with one of the $[(CH_3)_nNH_{4-n}]^+$ (n = 1–3) ions; (c) $(CH_3NH_3)_2SnCl_6$; (d) $[(CH_3)_2NH_2]_2SnCl_6$; and (e) $(NH_4)_2SiF_6$, which is isomorphous with $(NH_4)_2SnCl_6$. We have determined the magnetic symmetry and the spin Hamiltonian parameters of the thermally produced paramagnetic species. We discuss the structures of these paramagnetic species and the mechanisms of the solid-state chemical reactions.

Yu and Chou (*1*) have recently investigated via EPR thermal reduction of the type Cr(VI)O_4^{2-} → Cr(III) in single crystals of $(NH_4)_2SO_4$ and $LiNH_4SO_4$. This solid-state reaction can be regarded as the reduction part of an overall redox reaction. Wu and Yu (*2*) have recently investigated via EPR

0022-4596/92 $5.00

thermal reduction of the type $CrO_4^{2-} + e^- \rightarrow CrO_4^{3-}$ in $(NH_4)_3H(SeO_4)_2 : CrO_4^{2-}$ crystals. The ammonium ion, NH_4^+, is capable of acting as a reducing agent for the chromate ion in ammonium-containing compounds. We have now extended this type of investigation to other hydrogen-containing ions, such as the $[(CH_3)_nNH_{4-n}]^+$ (n = 1–3) ions, which could thermally reduce the chromate ion in solids. The monomethylammonium ion, $(CH_3NH_3)^+$, is abbreviated as $(MA)^+$; the dimethylammonium ion, $[(CH_3)_2NH_2]^+$, as $(DMA)^+$; and the trimethylammonium ion, $[(CH_3)_3NH]^+$, as $(TMA)^+$. The reducing agents described above are present in the host compounds either as a constituent or a dopant. However, we have found that identical thermal reductions can be accomplished in $K_2SnCl_6 : CrO_4^{2-}$ crystals coated with a thin layer of either $CH_3NH_2 \cdot HCl$ or NH_4Cl. The same thermal reductions can also be achieved by putting the crystals inside a powder mass of either $CH_3NH_2 \cdot HCl$ or NH_4Cl. These results shed light on the mechanisms of the solid-state reactions, and also provide a new method of hydrogenation for the solid state compounds.

The hydrogens, which participated in the thermal reduction of Cr(VI), could belong to a reducing molecule which is either a nearest neighbor to the chromate ion or far removed from it. In hydrogen-containing compounds, it is difficult to ascertain whether the hydrogen in question originated from a local or a nonlocal reducing ion. However, the fact that the thermal reductions in question can be achieved via reducing agents highly diluted in the crystals implies that the hydrogens originated from nonlocal reducing ions. Furthermore, since the same paramagnetic species are thermally produced by employing different reducing ions, it can be inferred that it is the hydrogens rather than other fragments of the reducing ions which are responsible for the observed solid-state reactions. That the same thermal reductions are experimentally observed by the method of coating with either $CH_3NH_2 \cdot HCl$ or NH_4Cl is consistent with this picture.

Chemical reactions in the solid state are apparently different from those in the liquid state. The solid-state reactions described in this paper are worthy of investigations in their own right. Besides, the methods described in this paper provide a new way of impurity doping. The conventional method for producing the CrO_4^{3-} species in solid state compounds is via X- or γ-ray irradiation of CrO_4^{2-}-doped crystals. However, the Cr(V) oxyanion species such as the CrO_4^{3-} and the CrO_3^- species produced via irradiation usually exist as several chemically inequivalent species. This is true for the Cr(V) oxyanions produced via γ-ray irradiation in $K_2SnCl_6 : CrO_4^{2-}$ and $(NH_4)_2SnCl_6 : CrO_4^{2-}$ crystals. On the other hand, the thermal method yields one chemical species. Therefore, the thermal method is more convenient and "cleaner" than the conventional method. Furthermore, the paramagnetic species can be produced in a controllable and repeatable manner.

The crystal structures of the M_2SnCl_6 compounds are simple and of high crystallographic point symmetries, including the cubic and the trigonal symmetries. These properties facilitate the determination of the magnetic symmetries and occupation sites of the thermally produced paramagnetic species. After the dissociation of the doped CrO_4^{2-} ion, the thermally produced Cr^{3+} ions may be forced to move away from the anionic site occupied by the chromate complex. In crystals of low point symmetry, it may not be easy to ascertain the occupation sites of the thermally produced Cr^{3+} ions. Furthermore, CrO_4^{2-} ions with relatively high concentration can be doped into the M_2SnCl_6 crystals. Consequently, M_2SnCl_6 crystals provide excellent hosts for the investigations of the solid-state reactions described in this paper.

Experimental

Single crystals of $(NH_4)_2SnCl_6$, K_2SnCl_6, and their solid solutions doped with the chromate ion were grown at 40 or 50°C, from slightly acidic aqueous solutions made up of stoichiometric amounts of $NH_4Cl(KCl)$ and $SnCl_4$. The crystal shape is predominantly octahedral for these cubic crystals; the {111} type faces are invariably obtained, and the {001} type faces are rare. $(MA)_2SnCl_6$: CrO_4^{2-} crystals were grown in a similar manner at 20 or 40°C. The crystals obtained for this trigonal compound were mainly the {0001} hexagonal plates. $(DMA)_2SnCl_6$: CrO_4^{2-} crystals which are of orthorhombic structure were also grown in a similar manner at 20 or 40°C. Some of the crystals obtained were (010) rectangular plates, which are useful for EPR measurements.

Thermal treatments of the M_2SnCl_6: CrO_4^{2-} crystals were carried out in a programmable furnace, usually at temperatures well below the decomposition temperature of the host compound. The EPR spectrometer used in this investigation has been described previously (*1*). Thermal decomposition of the host compound was investigated by using the DuPont 9900 series thermal analyzers. These included Thermalgravimetry Analysis (TGA) and Differential Thermal Analysis (DTA).

Crystal Structure of M_2SnCl_6

K_2SnCl_6, $(NH_4)_2SnCl_6$, and $(TMA)_2SnCl_6$ crystallize in the cubic $Fm3m$, K_2PtCl_6 structure (*3*). Figure 1 depicts the arrangement of atoms within a unit cell of the cubic K_2PtCl_6 lattice. $(MA)_2SnCl_6$ crystallizes in a rhombohedral ($R\bar{3}m$) distortion of the cubic K_2PtCl_6 structure (*3*). $(DMA)_2SnCl_6$ crystallizes in an orthorhombic (C_{2v}^7) distortion of the cubic K_2PtCl_6 structure (*4*). The basic crystallographic data of M_2SnCl_6 are summarized in Table I.

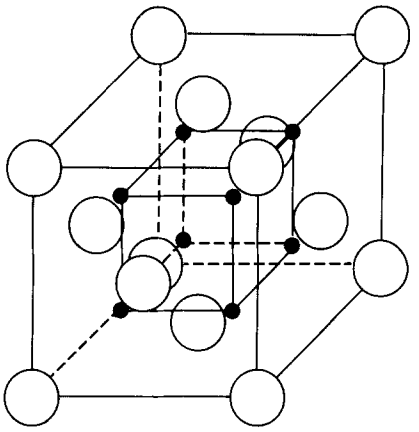

FIG. 1. A drawing depicting the atomic positions in cubic K_2PtCl_6 structure. The black circles denotes the cation and the large open circles the anion. The chlorines of the octahedral $(PtCl_6)^{2-}$ complex are located at special positions at the three cubic axes and equivalent positions.

Results and Discussion

A. Thermal Analysis

TGA results are summarized in Table II and plotted in Fig. 2. The measured weight

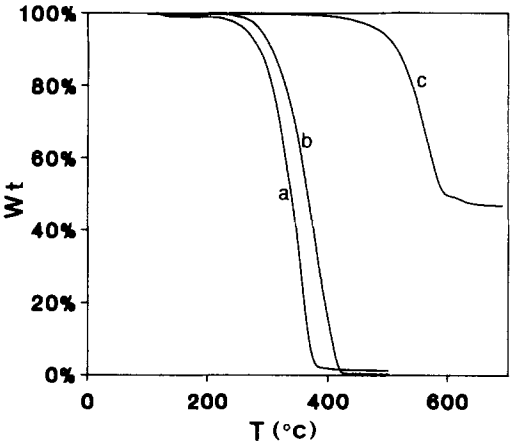

FIG. 2. The TGA curve for (a) $(CH_3NH_3)_2SnCl_6$, (b) $(NH_4)_2SnCl_6$, and (c) K_2SnCl_6. The curve for $[(CH_3)_2NH_2]_2SnCl_6$ almost coincides with that for $(CH_3NH_3)_2SnCl_6$.

TABLE I

THE BASIC CRYSTALLOGRAPHIC DATA OF M_2SnCl_6

Compound	Crystal system	Space group	Site symmetry				
			K	N	C	Sn	Cl
K_2SnCl_6	Cubic	$Fm3m$	$\bar{4}3m$			$m3m$	$4mm$
$(NH_4)_2SnCl_6$	Cubic	$Fm3m$		$\bar{4}3m$		$m3m$	$4mm$
$(CH_3NH_3)_2SnCl_6$	Trigonal	$R\bar{3}m$		$3m$	$3m$	$\bar{3}m$	m
$[(CH_3)_2NH_2]_2SnCl_6$	Orthorhombic	Pmn		m	m	m	m; 1
$[(CH_3)_3NH]_2SnCl_6$	Cubic	$Fm3m$		$\bar{4}3m$	$3m$	$m3m$	$4mm$

versus temperature data were taken at a rate of 10°C/min. TGA curves for the pure and the chromate-doped M_2SnCl_6 showed no discernible difference. The temperature T_w in Table II is defined as the temperature at which a 1% weight loss had been measured. The thermal treatment temperatures employed for the sample crystals were mostly well below the T_w of the compound, such that any thermal decomposition of the host compound should be minimal.

B. The Cr(VI) → Cr(V) Thermal Reduction in $(NH_4)_2SnCl_6 : CrO_4^{2-}$

The Cr(VI) → Cr(V) reduction can be accomplished via thermal treatment at temperatures well below the T_w of the host compound. For example, at 170°C for 8 hr or at 200°C for 1–4 hr. Crystals so treated yielded an $S = \frac{1}{2}$ paramagnetic species which can be identified as a Cr(V)($3d^1$) species. Figure 3 shows an [$\bar{1}$10]-oriented EPR spectrum at 120 K for this species. Figure 4 shows the observed and fitted (001) rotation patterns at 120 K. Each EPR line of this Cr(V) species displays an approximately 1 : 2 : 1 hyperfine pattern. $K_2SnCl_6 : CrO_4^{2-}$ crystals lightly (1%) co-doped with NH_4^+ and thermally treated yielded an identical $S = \frac{1}{2}$ EPR spectrum, but without a hyperfine pattern. Thus, this hyperfine pattern can be regarded as the result of the coupling of the odd electron of this Cr(V) species with two equivalent ammonium protons. $K_2SnCl_6 : CrO_4^{2-}$ crystals irradiated with γ-rays exhibited several Cr(V) species (see Section D). The symmetry and principal g-values of one of these species are identical to those of the thermally produced Cr(V) species in

TABLE II

THE DECOMPOSITION TEMPERATURE OF M_2SnCl_6

Compound	T_w (°C)
K_2SnCl_6	409
$(NH_4)_2SnCl_6$	225
$(MA)_2SnCl_6$	250
$(DMA)_2SnCl_6$	239
$(TMA)_2SnCl_6$	239

Note. T_w is defined as the temperature at which a 1% weight loss had occurred.

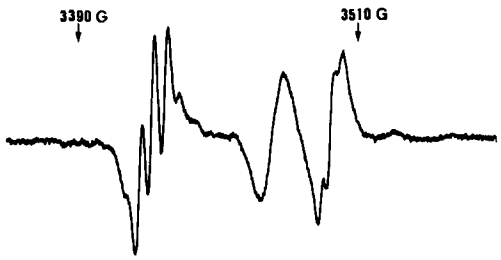

FIG. 3. A 120 K, [$\bar{1}$10] EPR spectrum of the Cr(V) species thermally produced in $(NH_4)_2SnCl_6$. The microwave frequency was about 9.5 GHz (same for the other figures).

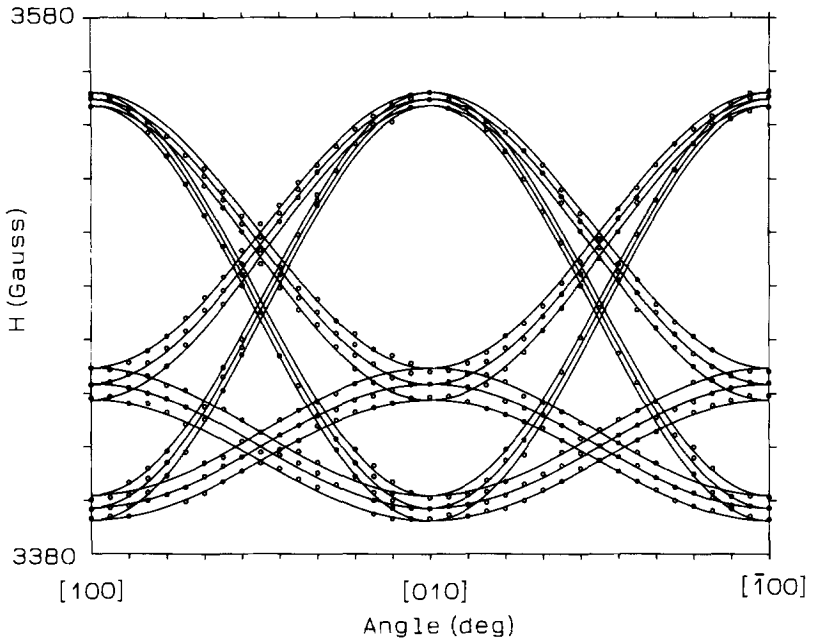

FIG. 4. The observed and fitted (001) rotation patterns at 120 K for the thermally produced Cr(V) species in $(NH_4)_2SnCl_6$.

$(NH_4)_2SnCl_6$ and K_2SnCl_6. The γ-ray produced Cr(V) species in K_2SnCl_6 does not exhibit the proton hyperfine structure. The absence of the detectable proton hyperfine structure for the thermally produced Cr(V) species in K_2SnCl_6 can be understood as a result of the diluteness of the doped NH_4^+ group.

The EPR spectrum of this Cr(V) species shows rhombic symmetry, with the three cubic axes of the host lattice as the principal axes of the spin Hamiltonian tensors. The rotation patterns can be analyzed by using the following effective g-factor for an $S = \frac{1}{2}$ species (*4*),

$$R^2 = l^2T_{xx} + m^2T_{yy} + n^2T_{zz} + 2lmT_{xy} + 2mnT_{yz} + 2nlT_{zx}, \quad (1)$$

where the 3×3 T_{ij} matrix is the square of the g-matrix, and l, m, n are the direction cosines of the magnetic field with respect to the reference axes which are chosen as parallel to the three cubic axes of the host lattice. The principal g-values and proton hyperfine constants used to fit the rotation patterns are listed in Table III.

C. The Cr(VI) to Cr(V) Thermal Reduction in K_2SnCl_6 Co-doped with NH_4^+

No EPR spectrum related to Cr(V) or Cr(III) can be detected from K_2SnCl_6: CrO_4^{2-} crystals thermally treated at temperatures below or above the T_w of the compound. However, the Cr(VI) to Cr(V) thermal reduction can be detected in K_2SnCl_6 crystals lightly codoped with $(NH_4)_2SnCl_6$. For example, a crystal co-doped with 1 mole% of $(NH_4)_2SnCl_6$ yielded a Cr(V) species with principal g-values identical to those of the Cr(V) species in $(NH_4)_2SnCl_6$, after it had been thermally treated at 200°C for 4 hr. This spectrum, however, did not show a clearly discernible proton hyperfine pattern. This shows that the ammonium ion

TABLE III

THE PRINCIPAL g-VALUES AND PROTON HYPERFINE CONSTANTS OBSERVED FOR THE Cr(V) SPECIES THERMALLY PRODUCED IN $(NH_4)_2SnCl_6$ AND IN AMMONIUM-DOPED K_2SnCl_6, AND γ-RAY PRODUCED IN K_2SnCl_6

Host	g_1	g_2	g_3	A_1 (G)	A_2 (G)	A_3 (G)	T (K)	Note
$(NH_4)_2SnCl_6$	1.996	1.969	1.910	5.9	4.7	2.5	120	Thermally produced
K_2SnCl_6	1.996	1.969	1.906				120	γ-ray produced
$K_2SnCl_6:NH_4^+$ (1%)	1.995	1.968	1.906				120	Thermally produced

is the reducing agent responsible for the Cr(VI) to Cr(V) thermal reduction in $(NH_4)_2SnCl_6$ and in ammonium-doped K_2SnCl_6.

D. Nature of the Thermally Produced Cr(V) Species

The thermally produced Cr(V) species could be one of the following four entities: (a) a CrO_4^{3-} tetrahedral complex; (b) a CrO_3^- complex; (c) an isolated Cr^{5+} ion; and (d) a Cr(V) oxychloride complex. It is known that via X- or γ-ray irradiation, the CrO_4^{2-} ion in solids can be reduced to either CrO_4^{3-} or CrO_3^-. The EPR of CrO_4^{3-} has been extensively studied in the past. The EPR of CrO_4^{3-} primarily in phosphate compounds has been reviewed by Greenblatt (*5*), and in the KH_2PO_4-type ferroelectrics by Dalal (*6*). We have undertaken EPR investigations of the Cr(V) oxyanions produced by γ-ray irradiation (total dosage of ca. 5 MRad) in chromate-doped $(NH_4)_2SnCl_6$ and K_2SnCl_6 crystals. In each case, several $S = \frac{1}{2}$ species, which can be construed as the Cr(V) oxyanions, were detected by EPR at liquid-nitrogen temperature. The EPR spectrum is additionally complicated by the presence of proton hyperfine lines in the ammonium compound and additionally by the presence of a large number of magnetically inequivalent sites. The EPR spectrum of the Cr(V) oxyanions produced by γ-ray irradiation in $K_2SnCl_6:CrO_4^{2-}$ is simpler, because of the absence of a proton hyperfine pattern. Upon comparing the observed (111) rotation patterns at 120 K, it becomes immediately clear that one of the γ-ray produced Cr(V) oxyanion species corresponds exactly to the thermally produced Cr(V) species in K_2SnCl_6 doped with the ammonium ion. Figure 5 shows the observed and fitted (111) patterns at 120 K for this γ-ray produced Cr(V) oxyanion species. This eliminates the possibility that the thermally produced Cr(V) species is a Cr^{5+} ion per se.

We consider next the Cr(V) oxychloride possibility. Earlier studies have reported on two Cr(V) oxychloride complex ions, namely $[CrOCl_4]^{-1}$ and $[CrOCl_5]^{-2}$; both of which have been studied by EPR. EPR of $[CrOCl_5]^{2-}$ has been reported by Kon and Sharpless (*7, 8*), and EPR of $[CrOCl_4]^{-1}$ has been reported by Garif'yanov (*9*). The spin Hamiltonian parameters have been tabulated in a review article by Goodman and Raynor (*10*). The EPR spectra of these two Cr(V) oxychlorides show axial symmetry, and their principle g-values are not similar to the thermally produced Cr(V) species in M_2SnCl_6. Furthermore, the EPR spectrum of $[CrOCl_5]^{2-}$ exhibited Cl hyperfine pattern (*8*), whereas that of the thermally produced Cr(V) species did not,. Therefore, it is very unlikely that the thermally produced Cr(V) species is one of these two Cr(V) oxychlorides.

The thermally produced Cr(V) species in M_2SnCl_6 ($M = K^+$ or NH_4^+) is then most likely to be either a CrO_4^{3-} tetrahedral complex or a CrO_3^- complex. The observed prin-

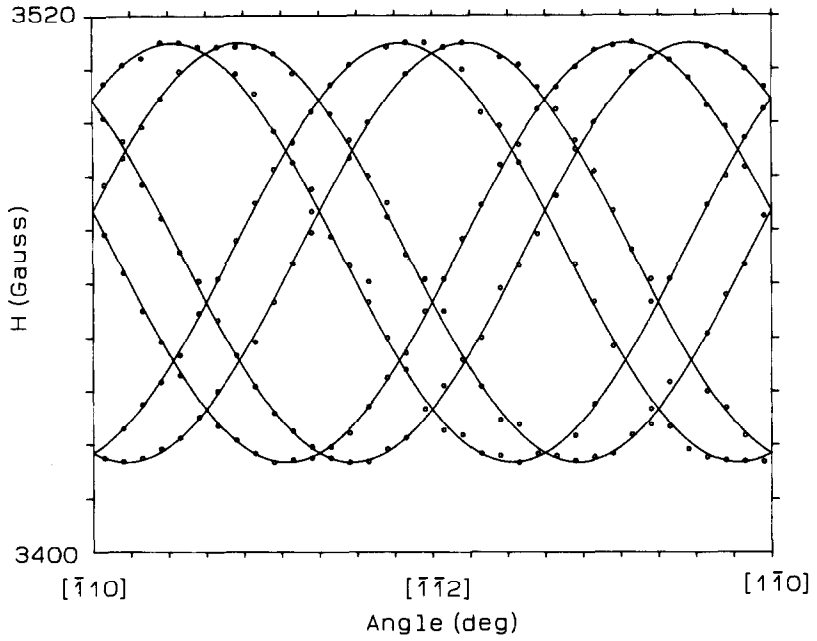

FIG. 5. The observed and fitted (111) rotation patterns at 120 K for one of the Cr(V) oxyanions produced by γ-ray irradiation in K_2SnCl_6.

cipal g-values indicates that the odd electron of the species is primarily localized in a $3d$ $x^2 - y^2$ orbital. It has been pointed out by Maple and Dalal (*11*) that it is difficult to distinguish between these two Cr(V) oxyanions simply from the evaluated principal g-values. They have proposed a relaxation method to resolve this difficulty. However, we will use a different approach to identify the nature of the thermally produced Cr(V) species. There is no experimental evidence which points out a mother–daughter relationship between the CrO_4^{3-} and the CrO_3^- species produced by X- or γ-ray irradiation. The CrO_3^- species appear to be independently produced, when a Cr–O bond was broken by the incident x- or γ-ray photon. If the thermally produced Cr(V) species is a CrO_3^- species, then it is a product of a redox reaction between the thermally excited chromate oxygens and the ammonium hydrogens. We note that the thermally produced Cr(V) species in question is the only Cr(V) species produced in M_2SnCl_6. It does not have another Cr(V) species as a precursor. This suggests that it is a CrO_4^{3-} rather than a CrO_3^- species (*1*).

E. Thermally Produced Cr(III) Species in $(NH_4)_2SnCl_6 : CrO_4^{2-}$

After $(NH_4)_2SnCl_6 : CrO_4^{2-}$ crystals are thermally treated at 300–320°C for 12–18 min (with approximately a 150°C/hr heating and cooling rates), two $S = \frac{3}{2}$ species which can be construed as Cr(III) species can be detected by EPR. When thermally treated at temperatures lower than T_w (such as at 170°C, described in Section B), the $-\frac{1}{2} \rightarrow +\frac{1}{2}$ transitions of these two $S = \frac{3}{2}$ species can be detected by EPR, along with the Cr(V) species. This indicates that the Cr(VI) → Cr(III) reduction can be accomplished in this compound via thermal treatments at temperatures lower than T_w. Figure 6 shows an EPR spectrum of these two thermally produced Cr(III) species. The EPR spec-

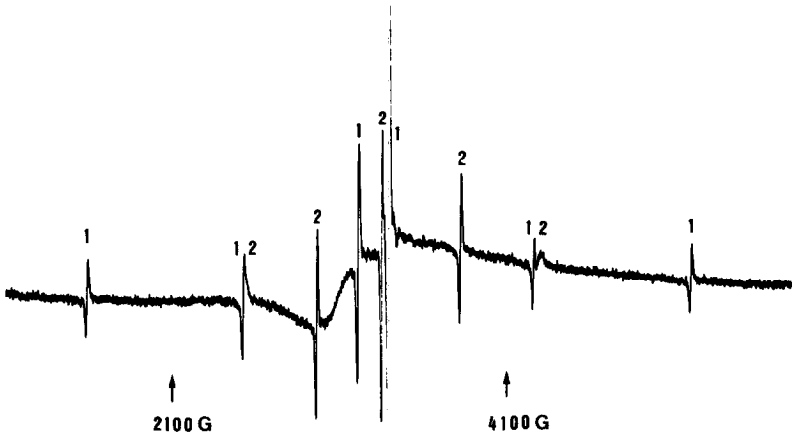

FIG. 6. A room-temperature, [100] EPR spectrum of the two tetragonal Cr(III) species thermally produced in $(NH_4)_2SnCl_6$. The EPR lines of Cr^{3+}(I) are marked by the numeral 1, and those of Cr^{3+}(II) by the numeral 2.

trum of either one of these two Cr(III) species had exhibited axial symmetry, with the symmetry axis pointing parallel to a cubic axis of the host lattice. The spectrum can be fitted by an $S = \frac{3}{2}$ spin Hamiltonian of the form,

$$\mathcal{H} = g\beta\mathbf{H}\cdot\mathbf{S} + D[S_z^2 - S(S+1)/3] + E(S_x^2 - S_y^2), \quad (2)$$

where the x, y, z axes refer to the principal axes of the crystal field. The secular equation for the energies of the ground state spin quadruplet can be written as (*12*)

$$W^4 - W^2[(\tfrac{5}{2})G^2 + 2D^2 + 6E^2] + WG^2[2D - 6D^2\cos^2\theta - 6E\sin^2\theta\cos(2\varphi)] + (\tfrac{9}{16})G^4 + (\tfrac{1}{2})G^2[D^2 - 6D^2\cos^2\theta + 9E^2\cos(2\theta) + 12DE\sin^2\theta\cos(2\varphi)] + (D^2 + 3E^2)^2 = 0, \quad (3)$$

where W is the energy, $G = g\beta H$, and θ and φ are the polar angles of the magnetic field with respect to the principal axes. In case of axial symmetry, the parameter E in Eq. (2) or Eq. (3) vanishes. We designate the thermally produced Cr(III) with a larger D parameter as the Cr^{3+}(I), and the other as the Cr^{3+}(II). The observed and fitted (001) rotation patterns for these two Cr(III) species are shown in Fig. 7, and the fitting parameters are listed in Table IV. In addition to the EPR spectra of the two thermally produced Cr(III) species, a very strong EPR signal which is isotropic and displays a seven-line structure (see Fig. 8) can be detected. The measured g-factor is 1.968, and the splitting between two adjacent lines of the seven-line structure is 2.6 G. This superhyperfine structure (SHFS) can be resolved only in the vicinity of a cubic axis. The measured intensity ratio of this seven-line pat-

TABLE IV

SPIN HAMILTONIAN PARAMETERS EVALUATED FOR THE THERMALLY PRODUCED Cr(III) IN M_2SnCl_6 AND $(NH_4)_2SiF_6$

Host	Species	g	D (G)	E (G)	T (K)
$(NH_4)_2SnCl_6$	I	1.986	896	0	120
	II	1.982	429	0	120
	III	1.986	0	0	120
$K_2SnCl_6:[(CH_3)_nNH_{4-n}]^+$	IV	1.981	949	0	300
$(MA)_2SnCl_6$	V	1.977	819	0	200
	VI	1.977	314	0	200
	VII	1.975	2532	471	200
$(DMA)_2SnCl_6$	VIII	1.986	767	−293	120
$(NH_4)_2SiF_6:MA^+$	IV	1.971	304	0	300

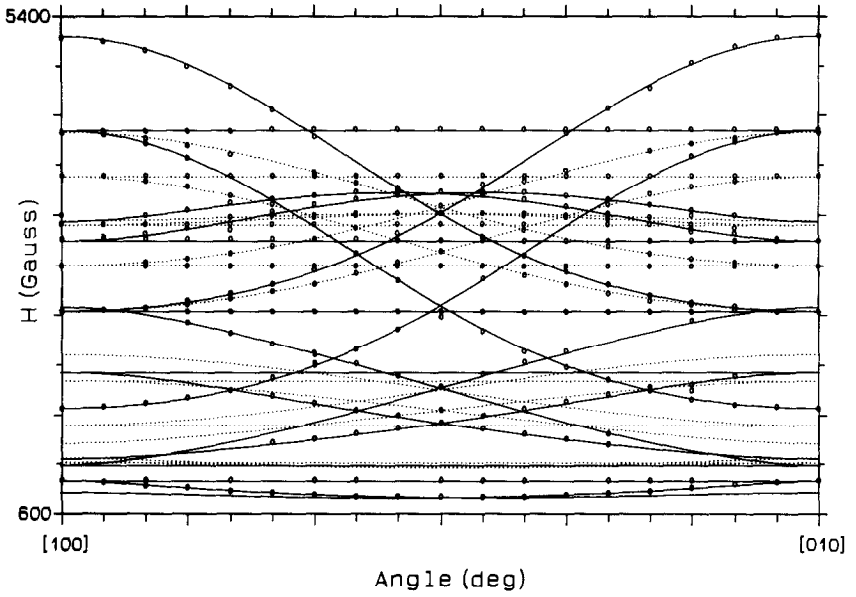

FIG. 7. The observed and fitted (001) rotation patterns at 120 K for the two thermally produced Cr(III) species in $(NH_4)_2SnCl_6$. The calculated fields of Cr^{3+}(I) are plotted as solid curves and those of Cr^{3+}(II) as broken curves.

tern corresponds to that expected for a SHF coupling to two equivalent $I = \frac{3}{2}$ (chlorine) nuclei. The chlorine splitting is small such that the isotope effect is not observable. The g-value of this species indicates that it could be either a Cr^{3+} or a Cr^{5+} ion. The orbital ground state of a Cr^{3+} ion in a cubic field of octahedral symmetry is a singlet, and the EPR spectrum is isotropic. Low (*13*) reported an isotropic EPR spectrum of Cr^{3+} ions with $g = 1.9800$ in MgO crystals. The orbital ground state is either a doublet or a triplet for a Cr^{5+} ion in a cubic crystal field. In either case, Jahn–Teller effect is expected to be operative. To our knowledge, there has never been a report of isotropic EPR spectrum observed for Cr^{5+}. Based on these considerations, we believe that the species in question is a Cr^{3+} ion (we designate it as the Cr^{3+}(III) species), but we are unable to establish a convincing model for the structure of this species. This dilemma may be resolved by employing ENDOR to probe the ligands of this species.

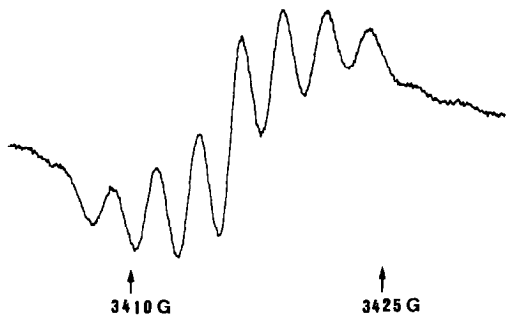

FIG. 8. The room-temperature, [100] EPR spectrum of a thermally produced Cr(III) species in $(NH_4)_2SnCl_6$. This EPR spectrum is isotropic and exhibits a seven-line SHFS.

F. Thermally Produced Cr(III) Species in K_2SnCl_6 Doped with $[(CH_3)_nNH_{4-n}]^+$

The Cr(VI) to Cr(III) reduction can be accomplished in K_2SnCl_6 doped with one of the $[(CH_3)_nNH_{4-n}]^+$ (n = 1–3) ions via

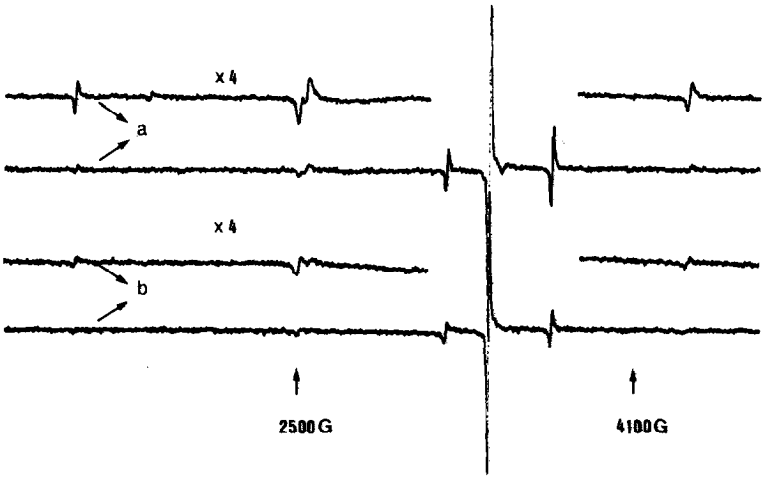

FIG. 9. The room-temperature, [$\bar{1}$10] EPR spectrum observed for a thermally produced Cr(III) species in K_2SnCl_6 doped with $(CH_3NH_3)^+$. The upper spectrum is for a crystal doped with a nominal 10 mole% of $(CH_3NH_3)_2SnCl_6$, and the lower spectrum for a crystal doped with a nominal 4 mole% of $(CH_3NH_3)_2SnCl_6$.

thermal treatment at temperatures much below T_w. Figure 9 shows two [$\bar{1}$10]-oriented EPR spectra detected for K_2SnCl_6 crystals co-doped with CrO_4^{2-} and MA^+ (nominally 10 and 4%), after these crystals are thermally treated at 350°C for 2 hr. The strong line in the EPR spectrum is isotropic with $g = 1.968$ and displays a seven-line SHFS with a splitting of 2.5 G. This SHFS can be resolved only in the vicinity of a cubic axis. The identity of this paramagnetic species should be similar to that of the Cr^{3+}(III) in $(NH_4)_2SnCl_6$. The rest of the EPR lines can be fitted as to belong to a Cr(III) species. Figure 10 shows the observed and fitted (111) rotation patterns for this Cr(III) species in K_2SnCl_6 crystals doped with a nominal 10 mole% of $(MA)_2SnCl_6$. The EPR spectra can be fitted by assuming that this $S = \frac{3}{2}$ species possesses axial symmetry, with the symmetry axis aligned parallel to a cubic axis of the host lattice. The evaluated spin Hamiltonian parameters are listed in Table IV. We designate it as the Cr^{3+}(IV).

Cr^{3+}(IV) can be thermally produced in K_2SnCl_6 crystals (doped with MA^+ in low concentration) at much lower temperatures. Figure 11 shows the observed [$\bar{1}$10] EPR spectrum for K_2SnCl_6 crystals doped with a nominal 2% of MA^+ and treated at 150°C ($\ll T_w$) for 15 hr. The two EPR lines marked with triangles correspond to the two $-\frac{1}{2} \rightarrow \frac{1}{2}$ transitions at [$\bar{1}$10] shown in Fig. 9. The strong line in Fig. 11 corresponds to a similar line in Fig. 9. Identical EPR spectrum (see Fig. 11) can be detected from similarly treated K_2SnCl_6 crystals doped with 4 mole% of $(DMA)_2SnCl_6$, or 4 mole% of $(TMA)_2SnCl_6$, but not for crystals doped with 5 mole% of $(NH_4)_2SnCl_6$ or 4 mole% of $[(CH_3)_4N]_2SnCl_6$. These show that in K_2SnCl_6 crystals, $[(CH_3)_nNH_{4-n}]^+$ (n = 1–3) are the much stronger reducing agents than NH_4^+. At low concentrations of the reducing agent, the doped chromate ion on the average would not be associated with one of the $[(CH_3)_nNH_{4-n}]^+$ ions. Hence, the fact that the Cr(VI) → Cr(III) reduction can be accomplished is significant. The implications of this experimental result is discussed in more details in Section K.

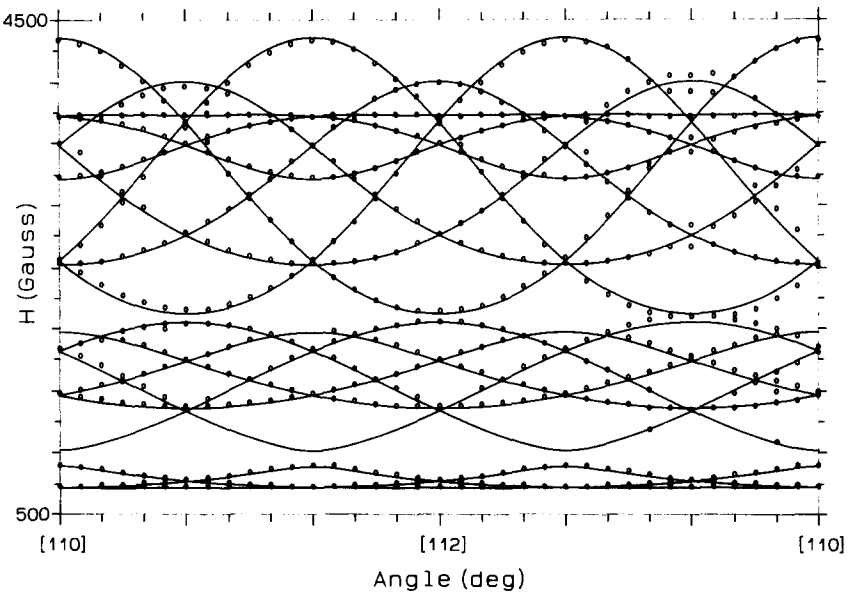

FIG. 10. The observed and fitted (111) rotation patterns at room temperature for the thermally produced Cr(III) species in K_2SnCl_6 crystals doped nominally with a 10 mole% of $(CH_3NH_3)_2SnCl_6$.

G. Thermally Produced Cr(V) and/or Cr(III) Species in $K_2SnCl_6 : CrO_4^{2-}$ Crystals Coated with Either $CH_3NH_2 \cdot HCl$ or NH_4Cl

The coating was made by dissolving $CH_3NH_2 \cdot HCl$ or NH_4Cl in ethanol and then by dipping the crystals into the solution and subsequently drying at 40°C. This process was repeated several times in order to get a thick enough layer of either $CH_3NH_2 \cdot HCl$ or NH_4Cl onto the crystals. As far as the thermal production of paramagnetic species is concerned, another method, which is equally effective, is simply to bury the crystals into dry powders of either $CH_3NH_2 \cdot HCl$ or NH_4Cl. After thermal treatments, the crystals were washed clean with ethanol.

After thermal treatment, the EPR spectrum exhibited by the crystals coated with $CH_3NH_2 \cdot HCl$ is identical to that exhibited by the crystals doped with MA^+. Namely, the thermally produced paramagnetic species are the Cr^{3+}(IV) and Cr^{3+}(III). In crystals coated with NH_4Cl or buried in NH_4Cl powder, the thermally produced Cr(III) species had exhibited an EPR spectrum identical to that exhibited by the crystals coated with $CH_3NH_2 \cdot HCl$ or buried in $CH_3NH_2 \cdot HCl$ powder. However, an $S = \frac{1}{2}$ species can also be detected at liquid-nitrogen temperature in crystals coated with NH_4Cl or buried in NH_4Cl, but not in crystals coated with $CH_3NH_2 \cdot HCl$ or buried in $CH_3NH_2 \cdot HCl$ powder. The EPR spectrum of this $S = \frac{1}{2}$ species is identical to that of the thermally produced Cr(V) oxyanion in $K_2SnCl_6 : CrO_4^{2-}$ crystals co-doped with NH_4^+. Thus this species can be identified as a CrO_4^{3-} species. Therefore, the effects of doping the $K_2SnCl_6 : CrO_4^{2-}$ crystals with NH_4^+ or $CH_3NH_3^+$ are identical to those of coating the crystals with NH_4Cl or $CH_3NH_2 \cdot HCl$. The only difference is this: The Cr^{3+}(IV) species can be thermally produced by the method of coating with NH_4Cl, whereas it cannot be produced by the method of doping

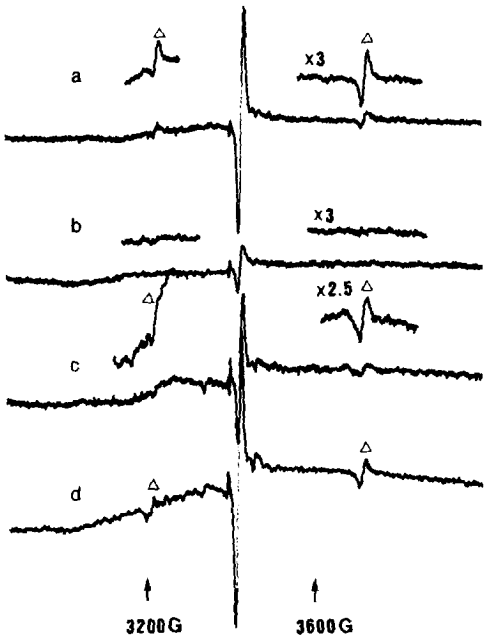

FIG. 11. The room temperature, [$\bar{1}$10] EPR spectrum observed for the thermally produced Cr(III) species in K_2SnCl_6 doped with one of the $[(CH_3)_nNH_{4-n}]^+$ (n = 0–3) ions. Only the $-\frac{1}{2} \rightarrow \frac{1}{2}$ transitions (marked with triangles) of the $S = \frac{3}{2}$ species can be observed. The strongest line is similar in nature to that shown in Fig. 8. Spectrum (a) is for a crystal doped with 2% of MA^+ and thermally treated at 150°C for 15 hr. Spectrum (b) is for a crystal doped with 5% of NH_4^+ and treated at 150°C for 15 hr. Spectrum (c) is for a crystal doped with 4% of $[(CH_3)_3NH]^+$ and treated at 150°C for 10 hr. Spectrum (d) is for a crystal doped with 4% of $[(CH_3)_2NH_2]^+$ and treated at 200°C for 2 hr.

with NH_4^+. This difference can be explained by the difference in the thermal fluxes of free hydrogens available for the Cr(VI) to Cr(III) thermal reduction.

H. Thermally Produced Cr(III) Species in $(MA)_2SnCl_6 : CrO_4^{2-}$

$(MA)_2SnCl_6 : CrO_4^{2-}$ crystals thermally treated at 120°C for 2 days did not yield any Cr(V) or Cr(III) species detectable by EPR. One rhombic and two axial Cr(III) species can be yielded by thermal treatments at 135°C for 8 hr or at 150°C for 15 hr. Thermally treated at 200°C for 2–4 hr yielded only the two axial Cr(III) species. The EPR spectra of these three thermally produced Cr(III) species can be analyzed by the spin Hamiltonian in Eq. (2), and the evaluated parameters are listed in Table IV. We designate the axial Cr(III) species with a larger D parameter as the Cr^{3+}(V), the other as Cr^{3+}(VI), and the rhombic species as Cr^{3+}(VII) (the rotation patterns for these three and other Cr^{3+} species are available upon request).

I. Thermally Produced Cr(III) Species in $(DMA)_2SnCl_6 : CrO_4^{2-}$

The Cr(VI) → Cr(III) thermal reduction can be carried out via thermal treatments at temperatures below T_w. The crystal structure of $(DMA)_2SnCl_6$ is of an orthorhombic distortion of the cubic K_2PtCl_6 structure (see Table II). A Cr(III) species can be detected by EPR in the crystals thermally treated at 180°C for 2 hr. The EPR spectrum shows rhombic symmetry, and can be analyzed by the spin Hamiltonian in Eq. (2). The evaluated spin Hamiltonian parameters are listed in Table IV. The a-axis is observed as a principal axis for the ligand field, and the other two principal axes lie on the bc plane. Figure 12 shows the observed and fitted resonance patterns at 120 K for rotations of the magnetic field about the three orthorhombic axes. We designate this species as the Cr^{3+}(VIII).

J. Thermally Produced Cr(III) Species in $(NH_4)_2SiF_6 : CrO_4^{2-}$

So far, it has been found that thermal reduction of the type Cr(VI) → Cr(V), or the type Cr(VI) to Cr(III) cannot be carried out in certain ammonium compounds. $(NH_4)_2SiF_6$ is one such example. $(NH_4)_2SiF_6$ crystallizes in two forms, a cubic and a trigonal modifications. The crystal structure of the cubic form is isomorphous with $(NH_4)_2SnCl_6$. Cubic $(NH_4)_2SiF_6 : CrO_4^{2-}$

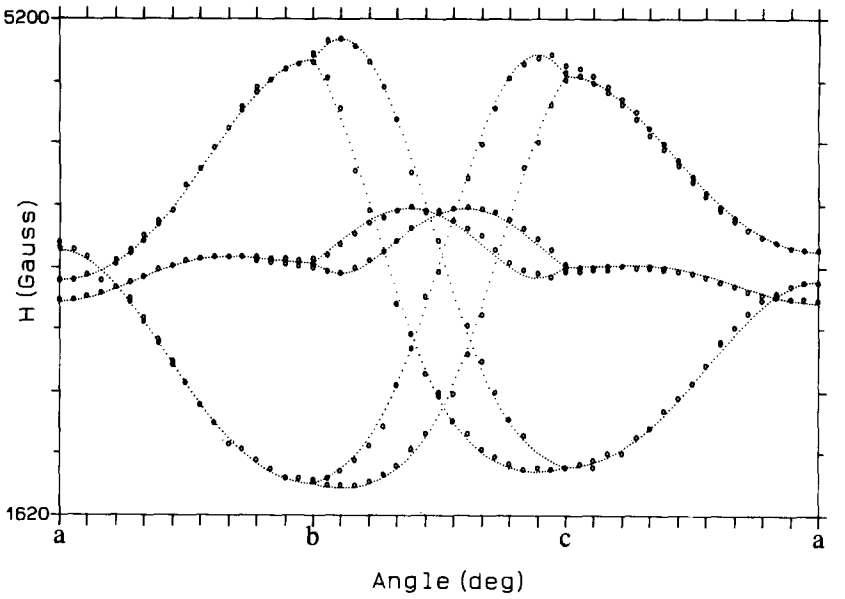

FIG. 12. The observed and fitted patterns at 120 K for rotations about the three orthorhombic axes for the thermally produced Cr(III) species in $[(CH_3)_2NH_2]_2SnCl_6$.

crystals were grown from aqueous solutions at 20°C. These crystals, after thermal treatments to the highest permissible temperature (about 300°C), did not yield any Cr(V) or Cr(III) species detectable by EPR. However, crystals co-doped with a nominal 4 mole% of $CH_3NH_2 \cdot HCl$ and thermally treated at 200°C for 1 hr yielded an EPR detectable Cr(III) species. Figure 13 shows a [100]- and a [110]-oriented EPR spectra observed at room temperature for this Cr(III) species. The EPR spectrum shows axial symmetry, with the symmetry axis aligned parallel to a cubic axis. The evaluated spin Hamiltonian parameters are listed in Table IV. We designate this Cr(III) species as the Cr^{3+}(IX). Apparently, in $(NH_4)_2SiF_6$, the reducing power of MA^+ is much larger than that of NH_4^+, which is also true in K_2SnCl_6.

K. Mechanism of the Cr(VI) to Cr(III) Thermal Reduction

The Cr(VI) to Cr(III) thermal reduction observed in chromate-doped M_2SnCl_6 crystals can be regarded as the reduction part of an overall redox reaction between the thermally excited chromate ion and the reducing ion. $Cr^{6+}(3d^0)$ is reduced to $Cr^{3+}(3d^3)$ and the hydrogens of the reducing ion is oxidized to H_2O. This thermal reduction can be accomplished in $K_2SnCl_6 : CrO_4^{2-}$ crystals doped with one of

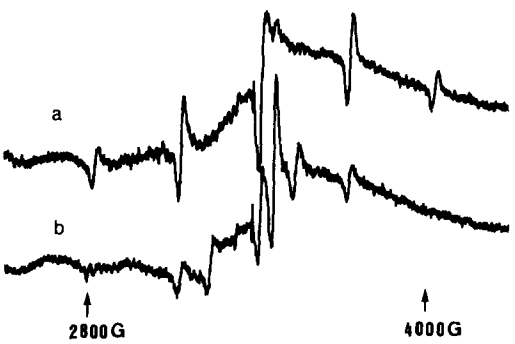

FIG. 13. The room-temperature EPR spectrum observed for a thermally produced Cr(III) species in $(NH_4)_2SiF_6$ doped with 4% of $CH_3NH_3^+$; (a) is at H// [100] and (b) at H//[110].

the $[(CH_3)_nNH_{4-n}]^+$ ions (n = 1–3). Furthermore, the Cr(III) species thermally produced are the same as those produced by employing different reducing ions, and the same is true for crystals coated with either $CH_3NH_2 \cdot HCl$ or NH_4Cl. However, this reduction cannot be detected in $K_2SnCl_6:CrO_4^{2-}$ crystals co-doped with the $[(CH_3)_4N]^+$ ion. These suggest that it is the hydrogens of the N–H groups rather than the C–H groups that are responsible for the observed thermal reduction, and that it is the protonic defect and the electronic defect associated with the thermally released free hydrogens rather than other fragments of the reducing ions which take part in the redox reaction.

The identity of the thermally produced Cr(III) species in M_2SnCl_6 could be an isolated Cr^{3+} ion or a Cr(III) oxychloride complex. We note that with the exception of the rhombic Cr(III) species in $(MA)_2SnCl_6$, the thermally produced Cr(III) species can be divided into two classes, in accordance with their zero-field splittings. The Cr^{3+}(I) in $(NH_4)_2SnCl_6$, the Cr^{3+}(IV) in K_2SnCl_6, and the Cr^{3+}(V) in $(MA)_2SnCl_6$ have exhibited axial symmetries and their D parameters are of the same order magnitude. We designate these species as the class A Cr(III) species. Likewise, the Cr^{3+}(II) in $(NH_4)_2SnCl_6$ and the Cr^{3+}(VI) in $(MA)_2SnCl_6$ can be put into the same class (class B). We note that only class A species can be thermally produced in $K_2SnCl_6:CrO_4^{2-}$ crystals and that the same Cr(III) species is thermally produced when the reducing ion MA^+ is located inside (doped) the host and outside (coated) the host. In the former (doped) case, some of the doped MA^+ ions could have completely thermally dissociated, thus creating cationic vacancies. Some of the thermally produced Cr^{3+} ions could have occupied an off-center cationic site. But this is not likely to happen in the latter case (coated). Based on these observations, we suggest that class A Cr(III) species are isolated Cr^{3+} ions occupying off-center (Sn^{4+}), interstitial sites. At the completion of the redox reaction, thermally produced Cr^{3+} ions are forced to move away from the anionic site occupied by the Cr^{6+} ion of the CrO_4^{2-} complex, to a nearby interstitial site at (0, 0, z) and equivalent positions in the cubic or trigonal host lattice. The site symmetry is either tetragonal or trigonal, and which could account for the axial symmetry observed for the EPR spectra. This class of Cr^{3+} ions could be associated with an H_2O molecule produced by the redox reaction. Such an H_2O molecule could occupy the lattice site vacated by the thermally dissociated CrO_4^{2-} complex. This arrangement of the H_2O molecule preserves the tetragonal or trigonal ligand arrangements. In this picture, the thermally produced Cr^{3+} ions are coordinated with one H_2O molecule and five Cl^- ions, but without forming a Cr(III) oxychloride complex. Garrett *et al.* (*14*) investigated the EPR of Cr^{3+} ions doped into single crystals of $(NH_4)_2[InCl_5(H_2O)]$. The doped Cr^{3+} ion is believed as to form a $[CrCl_5(H_2O)]^{2-}$ complex in this orthorhombic compound. The observed EPR spectrum is almost of axial symmetry. The spin Hamiltonian parameters reported by Garrett *et al.* are $g_\parallel = 1.9871$, $g_\perp = 1.9828$, $|D| = 594 \times 10^{-4}$ cm^{-1}, and $|E| = 50.7 \times 10^{-4}$ cm^{-1}. The zero-field splitting of this Cr(III) oxychloride complex is smaller than those of the class A Cr(III) species but larger than those of the class B Cr(III) species. Chlorine SHFS was not observed for the $[CrCl_5(H_2O)]^{2-}$ species (*14*), also unobservable for both class A and class B Cr(III) species. However, for the thermally produced Cr(III) species to be an oxychloride complex, it would require the participation of the $[SnCl_6]^{2-}$ complex in the redox reaction. But the same Cr(III) species is produced irrespective of the temperature of thermal treatments. Furthermore, symmetry consideration favors the model of isolated Cr^{3+} ions. We also suggest that

class B Cr(III) species be isolated Cr^{3+} ions occupying off-center cationic site in $(NH_4)_2SnCl_6$ or $(MA)_2SnCl_6$. We assume that at the completion of the redox reaction, some of the thermally produced Cr^{3+} ions migrate to an off-center, interstitial site near either an NH_4^+ or MA^+ vacancy created by thermal treatments. Attention, however, must be given to the tentative nature of these assignments. With ENDOR (which is not available to us) to probe its local environments, the structures of the thermally produced Cr(III) species could be established more confidently.

Acknowledgments

The authors thank Dr. S. Cheng of the Chemistry Department of the National Taiwan University for Thermal Analysis measurements, and are grateful for the support given by the National Science Council of the Republic of China during the period of this research.

References

1. J. T. Yu and S. Y. Chou, *J. Phys. Chem. Solids* **51,** 1255 (1990).
2. C. J. Wu and J. T. Yu, *J. Solid State Chem.* **93,** 549 (1991).
3. R. W. G. Wyckoff, "Crystal Structures," Vols. 3 and 5, Interscience, New York (1965).
4. N. M. Atherton, "Electron Spin Resonance," Wiley, New York (1973).
5. M. Greenblatt, *J. Chem. Educ.* **57,** 546 (1980).
6. N. S. Dalal, *Adv. Magn. Reson.* **10,** 119 (1982).
7. H. Kon and N. E. Sharpless, *J. Chem. Phys.* **42,** 906 (1965).
8. H. Kon and N. E. Sharpless, *J. Chem. Phys.* **43,** 1081 (1965).
9. N. S. Garif'yanov, *Dokl. Phys. Chem. Engl. Transl.* **155,** 249 (1964).
10. B. A. Goodman and J. B. Raynor, *Adv. Inorg. Chem. Radiochem.* **13,** 135 (1970).
11. S. R. Maple and N. S. Dalal, *J. Am. Chem. Soc.* **107,** 4082 (1985).
12. H. J. Gerristen, S. E. Harrison, H. R. Lewis, and I. P. Wittke, *Phys. Rev. Lett.* **2,** 153 (1959).
13. W. Low, *Phys. Rev.* **101,** 1827 (1956).
14. B. B. Garrett, K. DeArmond, and H. S. Gutowsky, *J. Chem. Phys.* **44,** 3393 (1966).